NRC Research Press

ARTICLE

Surface soil organic carbon in temperate and subtropical oriental oak stands of East China

Wenjuan Yu, Timothy J. Fahey, Hongzhang Kang, and Pisheng Zhou

Abstract: Forest ecosystems contain large amounts of soil organic carbon (SOC), which is a major component of biogeochemical cycles that may be sensitive to environmental change. We used a combination of nuclear magnetic resonance (NMR) spectroscopy and elemental and isotopic composition to examine the influence of soil properties and climatic factors on the quantity and degree of decomposition of SOC for organic and surface mineral horizons in seven oriental oak (*Quercus variabilis* Blume) forest sites arranged across a 11° latitudinal gradient in East China. Lacking Oa horizons, the two southernmost sites contained lower amounts of SOC in the forest floor horizon, but otherwise, latitudinal trends were not consistent. The SOC stock in the 0–10 cm mineral horizon exhibited no clear trend along the gradient and had a negative association with clay + silt content. Based on a higher alkyl/O-alkyl (A/O) ratio and alkyl/methoxyl (A/M) ratio, the SOC at the 0–10 cm depth appeared to be relatively more decomposed in three of the four southern subtropical sites. However, the degree of SOC degradation also decreased strongly with increasing soil pH ($R^2 = 0.90$, $P = 0.001$). Soil organic carbon exhibited increases in $\delta^{13}C$ and $\delta^{15}N$ and decreases in the C/N ratio with depth for all the seven sites, indicating an increase in its extent of decomposition. Our analysis indicated that the A/M ratio from NMR provided the best indication of the extent of SOC degradation along the latitudinal transect, whereas the elemental and isotopic composition better reflected patterns with soil depth.

Key words: soil organic matter, soil properties, climate, CP-MAS ^{13}C NMR, $\delta^{13}C$, $\delta^{15}N$.

Résumé : Les écosystèmes forestiers contiennent de grandes quantités de carbone organique du sol (COS) lequel est une composante majeure des cycles biogéochimiques qui peuvent être sensibles aux changements environnementaux. Nous avons combiné la spectroscopie de résonnance magnétique nucléaire (RMN) avec la composition élémentaire et isotopique pour étudier l'influence des propriétés du sol et des facteurs climatiques sur la quantité et le degré de décomposition du COS dans les horizons organique et minéral de surface dans sept stations de forêt de chêne oriental (*Quercus variabilis* Blume) réparties le long d'un gradient latitudinal de 11° dans l'est de la Chine. Ne comportant pas d'horizon Oa, les sols des deux stations les plus méridionales contenaient des quantités plus faibles de COS dans la couche holorganique mais les tendances latitudinales n'étaient par ailleurs pas consistantes. Le stock de COS dans l'horizon minéral de 0–10 cm ne montrait aucune tendance nette le long du gradient et avait une relation négative avec le contenu en argile + limon. Sur la base des ratios alkyle/O-alkyle (A/O) et alkyle/méthoxyle (A/M), le COS présent à une profondeur de 0–10 cm semblait relativement plus décomposé dans trois des quatre stations subtropicales situées au sud. Cependant, le degré de dégradation du COS diminuait aussi fortement avec l'augmentation du pH du sol ($R^2 = 0{,}90$, $p = 0{,}001$). Le COS montrait une augmentation du $\delta^{13}C$ et du $\delta^{15}N$ ainsi qu'une diminution du ratio C/N avec la profondeur dans toutes les stations, indiquant que le degré de sa décomposition augmentait. Notre analyse indique que le ratio A/M obtenu par RMN fournit la meilleure indication du degré de dégradation du COS le long d'un transect latitudinal tandis que la composition élémentaire et isotopique reflète mieux le profil en fonction de la profondeur dans le sol. [Traduit par la Rédaction]

Mots-clés : matière organique du sol, propriétés du sol, climat, RMN ^{13}C CP-MAS, $\delta^{13}C$, $\delta^{15}N$.

1. Introduction

Forest ecosystems in the Northern Hemisphere cover 2×10^9 ha and contain large amounts of carbon (C, 390 Pg), representing a huge reservoir of C on a global basis, mainly in the form of soil organic carbon (SOC, 260 Pg) (Goodale et al. 2002). Eswaran et al. (1993) estimated that 1576 Pg of organic carbon (OC) is stored in soils globally, with ~ 506 Pg (32%) of this in soils of the tropics, and ~40% of the C in soils of the tropics is in forest soils. Any change in the size and the turnover rate of soil C pools may potentially alter the atmospheric CO_2 concentration and the global climate (von Lützow et al. 2006).

Forest soil C storage is broadly associated with climate, management and disturbance history, tree species composition, microbial community composition and activity, and soil physical properties (Johnsen et al. 2013). For example, climate influences the accumulation and stabilization of soil C pools, as the biological activity that affects C turnover is temperature dependent (Pendall et al. 2004; Whitby and Madritch 2013). Tree species composition also has an important effect on the quantity and quality of SOC pools (Laganiere et al. 2013; Wang et al. 2013), e.g., by influencing soil microclimatic conditions (Hobbie et al. 2006) and by producing leaf and root litter in variable amounts and quality (Berg 2000). Xu et al. (2016) highlighted that clay content was the most important variable in regulating decomposition of SOC at a large scale (mean annual temperature ranging from –15 to 26 °C). Despite its pivotal role, our understanding of forest SOC and its controlling factors remains incomplete.

Received 20 August 2015. Accepted 10 February 2016.

W. Yu, H. Kang, and P. Zhou. School of Agriculture and Biology, Shanghai Jiao Tong University, 800 Dongchuan Rd., Shanghai 200240, China.
T.J. Fahey. Department of Natural Resources, Cornell University, G16 Fernow Hall, Ithaca, NY 14853-3001, USA.
Corresponding author: Hongzhang Kang (email: kanghz@sjtu.edu.cn).

Published at www.nrcresearchpress.com/cjfr on 11 February 2016.

Fig. 1. Distribution of the seven oriental oak forest sites along a 1500 km climatic gradient in East China. Three sites (PG, HYS, and BA) are in the warm temperate zone, and four sites (HZY, XY, HS, and YS) are in the subtropical zone.

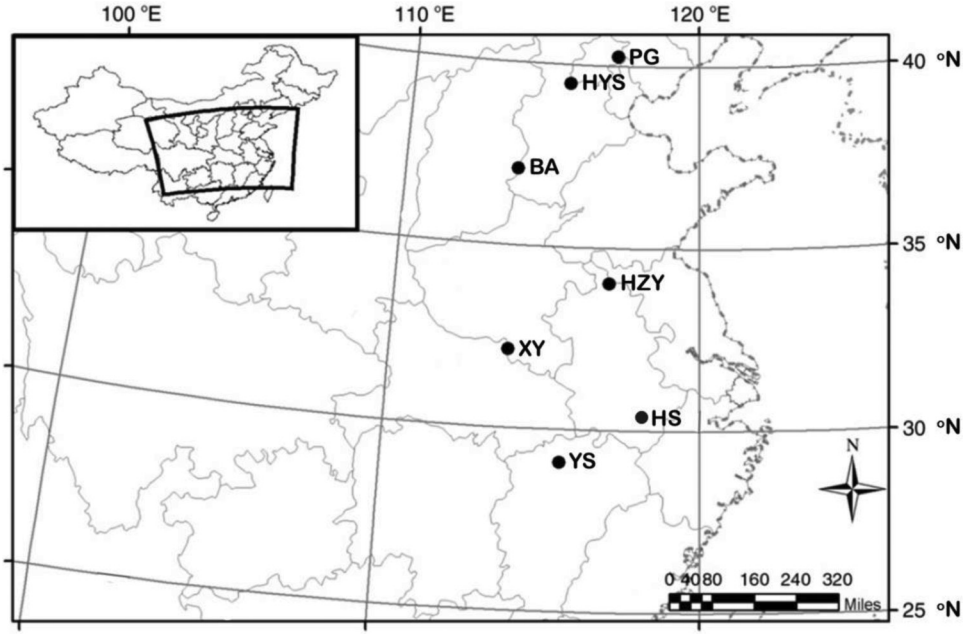

A variety of methods have been used to characterize the complex chemistry of SOC. Solid-state ^{13}C nuclear magnetic resonance with cross-polarization and magic angle spinning (CP-MAS ^{13}C NMR) provides a first approximation of the relative abundance of OC functional groups (Baldock et al. 1997; Clemente et al. 2012). The relative distributions of these broad C categories in SOC vary with decay (Yuste et al. 2012); for example, as the extent of degradation increases, the alkyl C spectral region increases concomitantly with the decrease in the O-alkyl C spectral region, and thus the alkyl/O-alkyl (A/O) ratio has been widely used to indicate the degree of organic matter decomposition (Baldock et al. 1997). Another indicator of the extent of SOC decomposition is the stable isotopic composition ($\delta^{13}C$), because reaction rates are slower for heavier isotopes than for lighter isotopes, enriching the remaining SOC with heavy isotopes (Guillaume et al. 2015). Indicating increases in stabilized SOC at greater soil depths, notably, both the A/O ratio and the $\delta^{13}C$ of SOC increase with depth in many soil profiles (Quideau et al. 2000; Garten 2006; Schneckenberger and Kuzyakov 2007). Using these methods, researchers have also observed that SOC may be less decomposed at higher latitudes, at least in subarctic zones (Norris et al. 2011; Sjogersten et al. 2003). To our knowledge, no such studies have been conducted comparing temperate and subtropical climatic zones.

In the present study, samples of the forest floor layers (Oe and Oa), as well as surface mineral soil horizons (0–2, 2–5, and 5–10 cm), were taken from seven oriental oak (*Quercus variabilis* Blume) forest sites in East China, three in the warm temperate climatic zone and four in the subtropical zone, and assessed by CP-MAS ^{13}C NMR, elemental, and isotopic analyses. Oriental oak is a common deciduous broadleaf tree species in East Asia (24°N–42°N and 96°E–140°E). Its distribution encompasses a wide range of annual temperatures and precipitations (Kang et al. 2011), providing a natural climatic gradient for studying SOC dynamics across two zones with control for tree species composition. We focused on the organic and surface mineral soil horizons, which contain large amounts of carbon that may be sensitive to environmental change (Du et al. 2014; Liski et al. 1999). The aims of this study were to (*i*) investigate SOC stock and concentration along the climatic gradient; (*ii*) investigate the degree of SOC decomposition, as indicated by CP-MAS ^{13}C NMR and $\delta^{13}C$ and $\delta^{15}N$, along both the latitudinal and depth gradients; and (*iii*) examine the role of soil properties and climatic factors determining SOC quantity and degree of decomposition along the gradient.

2. Materials and methods

2.1. Site descriptions

In July 2014, seven oriental oak stands were sampled across a large latitudinal range spanning 1500 km in East China, extending from Beijing (40.25°N, 117.12°E) to Jiangxi (29.09°N, 115.62°E) (Fig. 1). Three sites (PG, HYS, and BA) are located in the warm temperate zone based on the conventional boundary at 35°N latitude, and four sites (HZY, XY, HS, and YS) are located in the subtropical zone. All the sites are natural, second-growth, monospecific oriental oak stands that have not been disturbed by direct human activities and wildfires for at least the last five decades. Among the seven sites, only site HZY had an important herbaceous layer. Soils in the sites encompass three soil orders (USDA Soil Taxonomy): entisols at three sites (PG, HYS, and BA), inceptisols at two sites (HZY and XY), and ultisols at the most southerly sites (HS and YS). Climatic conditions of these sites change from cooler and drier in the north (mean annual temperature (MAT, °C), from 11.1 °C; mean annual precipitation (MAP, mm), from 492 mm) to warm and wet in the south (MAT, 16.9 °C; MAP, 1759 mm) (Table 1). Combining MAP and MAT, annual actual evapotranspiration (AET, mm) was estimated using the following equation (Ding 2013):

$$(1) \qquad AET = \frac{MAP}{\sqrt{[0.9 + (MAP \div E_0)^2]}}$$

where E_0 is the maximum annual potential of evapotranspiration with sufficient soil water (mm) that is calculated as $E_0 = 300 + 25MAT + 0.5MAT^3$.

2.2. Field sampling

At each site, forest structure was characterized in a 20 m × 20 m plot positioned at mid-slope in the study area, and canopy height and stem diameter at breast height (1.3 m) were measured for each tree (Table 1). Five parallel transects were established into each

Table 1. Selected climate, stand, and mineral soil characteristics at seven forest study sites composed of *Quercus variabilis* in China.

	Site						
Characteristic	PG	HYS	BA	HZY	XY	HS	YS
Latitude (°N)	40.25	39.48	37.09	34.02	32.12	30.12	29.09
Longitude (°E)	117.12	115.48	113.83	117.06	114.01	118.29	115.62
Altitude (m)	260	516	801	117	131	450	360
MAP (mm)	591	530	492	688	1045	1701	1759
MAT (°C)	11.5	11.1	12.7	14.9	15.2	16.1	16.9
AET(mm)	454	423	421	548	677	810	853
Stand density (stem·hm^{-2})	2267	3200	800	1422	1066	978	933
DBH (cm)	12.43	12.83	14.22	22.85	16.84	28.17	28.07
Basal area (m^2·hm^{-2})	29.15	43.69	17.20	60.01	24.84	70.52	61.93
Canopy height (m)	11.2	9.4	12.6	16	13.6	13.0	18
Clay (%)	23.8±1.6	20.4±0.8	13±0.3	34.3±0.9	16.7±0.9	26.8±1.4	29.2±0.6
Silt (%)	53.9±1.3	47.0±2.2	35.6±1.3	53.2±1.4	43.7±1.0	49.3±1.1	24.8±1.1
Sand (%)	22.3±0.3	32.7±1.8	51.4±1.5	12.5±0.7	39.6±1.5	23.9±1.3	46±0.5
pH (in water)	6.24±0.10	6.69±0.20	5.95±0.11	7.58±0.13	4.50±0.04	4.74±0.03	4.35±0.05
Soil density (g·cm^{-3})	0.93±0.04	0.99±0.03	1.01±0.04	1.26±0.02	1.02±0.05	0.93±0.02	0.98±0.03
C (%)	2.37±0.12	3.45±0.28	3.15±0.12	2.04±0.04	3.82±0.45	2.73±0.13	3.99±0.17
N (%)	0.22±0.01	0.28±0.02	0.27±0.01	0.18±0.00	0.28±0.03	0.22±0.01	0.30±0.01
Total OC stock (kg·m^{-2})	3.41±0.20	4.32±0.29	4.07±0.12	2.95±0.09	4.72±0.48	2.71±0.13	4.18±0.17

Note: The climatic data are an average of the last 5 years recorded by the local ecological stations. Values are given as mean ± standard error, with $n = 5$ (for soil density, $n = 15$). Total organic carbon (OC) stock includes both organic horizons and 0–10 cm mineral soil. MAP, mean annual precipitation; MAT, mean annual temperature; AET, annual actual evapotranspiration; DBH, stem diameter at breast height; C, carbon; N, nitrogen.

site with 10 m spacing between them and with 10 sampling points on each transect at 5 m spacing (i.e., 50 m × 50 m grid). The forest floor horizons (Oe and Oa) were collected with hand spades in a circle that was 13 cm in diameter to the top of the mineral soil; the boundary between forest floor and mineral soil was usually distinct, marked by high stoniness and by color and texture. Mineral soil samples were collected with a 2.5 cm corer at 0–2, 2–5, and 5–10 cm depths. For each of the five transects, the samples from the 10 points were composited by horizons. Oa horizons were not observed at the two southernmost sites, i.e., HS and YS.

Ten additional 2.5 cm diameter soil cores of the whole 0–10 cm mineral horizon were collected on each transect and composited by transect for measuring soil pH, %C, %N, and texture. Fifteen soil cores (three per transect) were excavated to 10 cm depth using a bulk density corer. Soil samples were placed in polyethylene bags, stored on ice, and transferred to the laboratory within 24 h. Mineral soils were sieved (2 mm), and the mass of the fine and coarse fractions was measured.

2.3. Soil physico-chemistry

Using the 0–10 cm bulk mineral soil, soil pH was measured at a soil to water ratio of 1:2.5 (*m*/*v*); soil particles were classified into silt, clay, and sand using the Bouyoucos hydrometer method (Elliott et al. 1999). Bulk density of the 0–10 cm mineral soil was calculated by dividing the dry mass (dried at 105 °C until constant mass) by the soil core volume (corrected with the volume of stones (>2 mm)). Forest floor C stock was calculated as the product of dry mass and C concentration, whereas 0–10 cm mineral soil C stock was estimated using the concentration data and bulk density measures, and both values were scaled to kilograms per metre squared. Both carbon stock and carbon concentration were used to indicate SOC quantity.

2.4. NMR analysis

Two of the five replicates for each depth and site were used for NMR analysis. Prior to NMR analysis, each of the 42 mineral soil samples (three depths × two replicates × seven sites) were treated with hydrofluoric acid to concentrate the organic matter and remove paramagnetic minerals (Simpson and Simpson 2012). About 5 g of the sample was shaken with 30 mL 10% hydrofluoric acid for 2 h. After centrifugation for 10 min, the supernatant was removed. The procedure was repeated five times. The remaining sediment was washed five times with 30 mL deionized water to remove residual hydrofluoric acid before freeze drying. Using two parallel samples, the CP-MAS ^{13}C NMR spectra for each mineral horizon at each site were acquired twice on a Bruker Avance 400 MHz NMR spectrometer, equipped with a 4 mm broadband CP-MAS probe. Approximately 100 mg of sample was packed into a 4 mm zirconium rotor with a Kel-F cap. The acquisition parameters were as follows: spectral frequency of 100.613 MHz for ^{13}C and 400.13 MHz for ^{1}H, spinning rate of 5 kHz, ramp-CP contact time of 1.5 millisecond, 1 s recycle delay, 17 128–10 0967 scans per sample, and exponential line broadening of 50 Hz. Glycine was used as an external standard to calibrate the chemical shifts.

After correcting the spinning sidebands of carboxyl carbon, the spectra were integrated using Topspin version 2.1 and assigned based on Mathers et al. (2007). Eight structural regions were integrated: alkyl carbon (0–45 ppm), N-alkyl/methoxyl carbon (45–60 ppm), carbohydrate carbon (60–90 ppm), di-O-alkyl carbon (90–110 ppm), aryl carbon (110–145 ppm), O-aryl carbon (145–165 ppm), carboxyl carbon (165–190 ppm), and ketone carbon (190–210 ppm). The alkyl region (0–45 ppm) contains carbon in compounds such as lipids, cutin, and suberin. The O-alkyl C region (45–110 ppm) typically corresponds to more easily degraded OM constituents such as those found in carbohydrates (Supplementary Fig. S1[1]) (Simpson and Simpson 2012). The alkyl/O-alkyl (A/O) ratio, which usually increases with progressive degradation, was calculated by dividing the area of the alkyl region (0–45 ppm) by the area of the O-alkyl region (45–110 ppm) (Simpson et al. 2008). The alkyl/methoxyl (A/M) ratio also was calculated based on the area of the alkyl region (0–45 ppm) and the N-alkyl/methoxyl region (45–60 ppm). Both the A/O and A/M ratios were used to indicate the degree of SOC decomposition.

[1]Supplementary data are available with the article through the journal Web site at http://nrcresearchpress.com/doi/suppl/10.1139/cjfr-2015-0324.

Fig. 2. Soil organic carbon stock (kg·m^{-2}) in organic and mineral layers in seven oriental oak stands. Values are given as mean ± standard error, with n = 5.

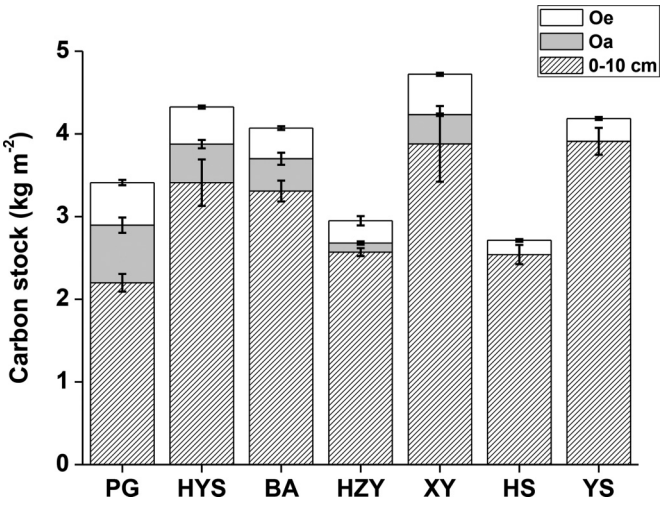

2.5. Elemental and isotopic analyses

The sieved mineral soil horizons were air-dried and the Oa and Oe horizons were dried at 65 °C until constant mass before isotopic analysis. The isotopic composition, total C, and total nitrogen (N) of these samples were measured on a Vario EL III Elemental Analyzer coupled to an Isotopic Ratio Mass Spectrometer (Elementar Analysensysteme GmbH, Germany). Elemental results were converted to an oven-dried mass basis. Isotopic results were expressed in the δ-notation, as the ‰ variation from the standard reference material, Pee Dee Belemnite (PDB) for C and atmospheric N_2 for N.

2.6. Statistics

Statistical tests were performed using the SPSS 19.0 software (SPSS Inc., Chicago, Illinois). Although the other data were calculated as arithmetic means of five replicates with standard errors, NMR data were calculated as arithmetic means of two replicates. To perform the following statistical methods, NMR compositions at the 0–10 cm depth were calculated by summing the weighted values of 0–2, 2–5, and 5–10 cm depths (i.e., multiplied by 0.2, 0.3, and 0.5, respectively).

A general linear model was applied to evaluate differences between climatic zones of carbon stock and the various indexes of degree of SOC decomposition. For 0–10 cm mineral horizon, Pearson correlations were used to evaluate the inter-relationships among the soil and climate variables. Stepwise multiple regression analyses were conducted to evaluate the effects of soil and climate factors on SOC concentration and degree of degradation, where MAP, MAT, and AET were included as climatic variables and clay + silt content and pH were included as soil properties.

3. Results

3.1. SOC concentration and stock

Forest floor OC stock differed significantly between zones (P < 0.001; Supplementary Table S1[1]). At the most southerly sites (HS and YS), where Oa horizons were lacking, forest floor OC stock was particularly low (0.17 and 0.28 kg·m^{-2}, respectively) and low forest floor OC stock was also observed at a third subtropical site (site HZY) that had a thin Oa horizon (Fig. 2). However, one of the subtropical sites (site XY) had comparatively well-developed forest floor horizons, similar to the temperate zone sites. The 0–10 cm mineral SOC stock exhibited no significant difference between climatic zones (P = 0.359) and did not show any clear trend with latitude (Fig. 2). Based on stepwise regression analysis, the only soil or climatic factor that had a significant effect on mineral soil OC concentration was silt + clay content. The percent C decreased with increasing silt + clay content across the seven sites (R^2 = 0.66, P = 0.026; Table 2).

Table 2. Stepwise multiregression analysis of soil organic carbon (SOC) quantity and composition with soil and climatic variables.

SOC quantity and composition	Variables entered	R^2	n	P	Regression
C concentration (%)	Clay + silt content	0.66	7	0.026	y = –0.04x + 5.94
A/O ratio	pH	0.73	7	0.014	y = –0.04x + 0.84
A/M ratio	pH	0.90	7	0.001	y = –0.37x + 5.25

Note: Variables used in the regression analysis: clay + silt content, pH value, mean annual temperature, mean annual precipitation, and annual actual evapotranspiration. For carbon (C) stock, none of the five variables entered into the model. A/O ratio, alkyl/O-alkyl ratio; A/M ratio, alkyl/methoxyl ratio.

3.2. SOC: NMR analysis

For the 0–10 cm mineral soil, the percentage of signal intensity attributable to alkyl C was significantly lower (P = 0.021) in the northern sites than in the southern sites (Table 3; Supplementary Table S1[1]). The percentage of alkyl C was significantly correlated with both pH and AET (Table 4). The relative contribution of methoxyl C to total signal intensity also was significantly different between zones (P = 0.038; Supplementary Table S1[1]) and generally higher in the northern sites than in the southern sites (Table 3); it was strongly correlated with pH and significantly correlated with MAP and AET (Table 4). The contributions of carbohydrate C, di-O-alkyl C, and the whole O-alkyl regions were neither significantly different between zones nor correlated with the environmental variables (Table 4; Supplementary Table S1[1]).

Neither index of degree of decomposition, the A/O and A/M ratios, showed any consistent trend with increasing soil depth (Table 3). However, averaged across the 0–10 cm mineral layer, both the A/O and A/M ratios decreased significantly with increasing soil pH (P < 0.05; Table 4), whereas no effect of soil texture (silt + clay content) was observed. The A/M ratio also was correlated with climatic variables, as significant positive relationships with MAP and AET were observed (P < 0.05; Table 4). Stepwise regression analysis also showed that pH was the most important variable in controlling the A/M ratio across these sites (R^2 = 0.90, P = 0.001; Table 2).

3.3. SOC: elemental and isotopic composition

The C/N ratios ranged from 10.16 in the 5–10 cm horizon of site PG to 30.16 for the Oe horizon at site HYS (Fig. 3*a*). The C/N ratios decreased with depth in the soil profiles and declined more dramatically in the forest floor than in the mineral soil. The $\delta^{13}C$ ranged from –28.38‰ in the Oe horizon at site YS to –17.63‰ for the 5–10 cm horizon at site HZY (Fig. 3*b*). For a given horizon, the values of $\delta^{13}C$ were higher in the northern sites than in the southern sites, with the striking exception of site HZY. The $\delta^{15}N$ ranged from –4.86‰ in the Oe horizon at site XY to 5.97‰ for the 2–5 cm horizon at site PG (Fig. 3*c*). Similar to $\delta^{13}C$ values, $\delta^{15}N$ values also showed a generally increasing trend with soil depth. However, no consistent trend was found for $\delta^{15}N$ values among sites within a given horizon.

4. Discussion

4.1. SOC quantity

We observed especially low forest floor carbon stocks in three of the subtropical oak forest stands (Fig. 2). Accumulation of SOC in surface organic layers is mainly driven by rates of C input (litterfall and fine root turnover), by the biochemical quality of litter, and by decomposition and mixing rates (Jandl et al. 2007). Focusing on one single tree species, the influence of litter quality was

Table 3. Soil organic carbon (SOC) composition (%) in different soil depths at seven study sites (arranged in order of decreasing latitude) using CP-MAS ^{13}C NMR.

Site	Depth (cm)	Alkyl	N-alkyl/ methoxyl	Carbohydrate	Di-O-alkyl	Aryl	O-aryl	Carboxyl	Ketone	A/O ratio	A/M ratio
PG	0–2	26.41	9.96	29.28	8.31	9.44	4.38	10.17	2.05	0.56	2.65
	2–5	24.41	9.89	30.28	8.46	9.36	4.19	11.16	2.25	0.50	2.48
	5–10	27.28	9.48	28.65	7.69	10.11	4.12	10.78	1.89	0.60	2.88
HYS	0–2	26.08	10.83	29.68	7.85	9.01	3.93	10.78	1.84	0.54	2.42
	2–5	28.20	11.03	30.00	7.47	8.83	3.13	10.22	1.13	0.58	2.57
	5–10	29.15	9.50	28.88	7.42	9.31	3.37	10.82	1.55	0.64	3.07
BA	0–2	27.76	10.28	29.84	7.77	8.54	3.70	10.26	1.85	0.58	2.70
	2–5	27.33	10.00	29.96	7.57	8.51	3.80	10.81	2.03	0.58	2.74
	5–10	27.25	9.03	30.54	7.98	9.43	3.42	10.49	1.85	0.57	3.02
HZY	0–2	24.85	10.31	30.95	8.65	8.33	4.08	10.69	2.15	0.50	2.41
	2–5	26.88	10.33	30.57	8.14	7.57	3.50	10.98	2.03	0.55	2.60
	5–10	27.63	10.11	31.07	8.08	7.56	3.02	10.88	1.65	0.56	2.73
XY	0–2	28.94	9.02	30.09	7.87	8.27	4.21	9.40	2.20	0.62	3.21
	2–5	30.62	8.19	29.40	7.74	8.33	3.63	9.94	2.15	0.68	3.75
	5–10	33.20	8.43	28.61	7.36	7.79	3.42	9.32	1.87	0.75	3.94
HS	0–2	27.55	9.49	34.65	8.46	6.87	2.52	9.12	1.34	0.53	3.00
	2–5	31.18	8.51	32.38	7.75	7.56	2.29	9.10	1.25	0.64	3.67
	5–10	30.21	8.54	32.99	7.59	7.76	1.92	9.71	1.28	0.62	3.54
YS	0–2	30.35	8.48	30.12	7.54	8.31	3.14	10.29	1.77	0.66	3.58
	2–5	28.94	8.85	29.84	7.61	8.79	3.00	11.05	1.93	0.63	3.29
	5–10	31.11	7.88	29.52	6.87	9.17	2.25	11.54	1.66	0.70	3.95
PG	0–10	26.25	9.70	29.27	8.04	9.75	4.19	10.77	2.03	0.56	2.71
HYS	0–10	28.25	10.22	29.38	7.52	9.10	3.41	10.63	1.48	0.59	2.79
BA	0–10	27.38	9.57	30.22	7.82	8.98	3.59	10.54	1.90	0.58	2.87
HZY	0–10	26.85	10.22	30.90	8.21	7.72	3.37	10.87	1.86	0.54	2.63
XY	0–10	31.58	8.48	29.15	7.57	8.05	3.64	9.52	2.02	0.70	3.74
HS	0–10	29.97	8.72	33.14	7.81	7.52	2.15	9.40	1.29	0.61	3.47
YS	0–10	30.31	8.29	29.73	7.22	8.89	2.66	11.14	1.76	0.67	3.68

Note: Values are given as the mean of two replicates. A/O ratio, alkyl/O-alkyl ratio; A/M ratio, alkyl/methoxyl ratio.

Table 4. Pearson correlations (*r*) among soil organic carbon (SOC) and soil and climatic variables across seven oak forest study sites in China ($N = 7$).

	Clay + silt content (%)	pH	MAT (°C)	MAP (mm)	AET (mm)
C stock (kg·m^{-2})	−0.75	−0.32	−0.17	−0.16	−0.12
C concentration (%)	−0.81*	−0.69	0.25	0.37	0.36
Alkyl C (%)	−0.41	−0.85*	0.67	0.72	0.76*
N-alkyl/methoxyl C (%)	0.47	0.97**	−0.75	−0.83*	−0.85*
Carbohydrate C (%)	0.37	−0.09	0.46	0.47	0.43
Di-O-alkyl C (%)	0.71	0.68	−0.30	−0.51	−0.47
O-alkyl C (%)	0.64	0.51	−0.03	−0.10	−0.14
A/O ratio (%)	−0.55	−0.86*	0.57	0.61	0.66
A/M ratio (%)	−0.45	−0.95**	0.75	0.82*	0.85*
Clay + silt content (%)		0.55	−0.06	−0.12	−0.08
pH			−0.61	−0.78*	−0.76*
MAT (°C)				0.86*	0.93**
MAP (mm)					0.98**

Note: **, $P < 0.01$; *, $P < 0.05$.MAT, mean annual temperature; MAP, mean annual precipitation; AET, annual actual evapotranspiration; C, carbon; A/O ratio, alkyl/O-alkyl ratio; A/M ratio, alkyl/methoxyl ratio.

minimized in the present study. Although we did not measure litterfall, all the stands had closed canopies, and in fact, the largest trees and highest forest basal area were found in the three subtropical sites with low forest floor carbon stock (Table 1); hence, it seems unlikely that low litterfall inputs explain this pattern. More likely, higher temperature and moisture accelerate soil organic matter decay and reduce the accumulation of SOC in the organic layer; for example, Meentemeyer (1978) demonstrated the dependence of litter decay on site evapotranspiration, and distinctly higher AET was estimated for the subtropical sites (Table 1). Another possible contributor might be soil invertebrates, e.g., earthworms and millipedes, that mix the forest floor into mineral soil (Nielsen and Hole 1964). Lin et al. (2009) observed that both the amount and diversity of forest floor macrofauna showed increasing trends from north to south in eight typical forest ecosystems across China. These increases might contribute to faster litter decomposition and a reduced stock of forest floor C in the south.

Carbon stock in surface mineral soil showed no clear trend along the latitudinal gradient (Fig. 2). The factors controlling the accumulation of SOC in mineral layers are more complex than in the organic layer. In addition to the degree of microbial processing, it also depends on both the aboveground and belowground C sources (Laganiere et al. 2013), as well as mechanisms of stabilization associated with clay minerals and aggregation (Schmidt et al. 2011). We found a significantly negative effect of clay + silt content (i.e., a positive effect of sand content) on SOC concentration. Carter et al. (1998) proposed that the capacity of a soil to protect and accumulate soil organic matter (SOM) in organomineral particles is not always positively related to the clay and silt content per se but rather to the degree to which this capacity level is filled. Once the clay + silt content is saturated with organic matter, additional SOM would be found in macroaggregates, possibly as sand-sized macro-organic matter (Carter 2002). Also, although we did not measure it, certain clay minerals, especially short-range ordered minerals, are particularly effective in SOC sequestration (Kögel-Knabner et al. 2008) and perhaps the proportion of these minerals differs among the sites. We also found a weak negative relationship between pH and mineral soil C concentration ($R^2 = 0.48$, $P = 0.085$). One possible explanation might be that SOC had a higher solubility at high pH (Yin et al. 1996; Tavakkoli et al. 2015), and more dissolved OC could lead to the reduced accumulation of SOC. Our findings suggested that soil properties such as texture and pH were closely associated with SOC accumulation.

Fig. 3. Elemental and isotopic composition of organic matter in forest floor and mineral soils in oriental oak stands along the latitudinal gradient. (*a*) C/N ratio, (*b*) $\delta^{13}C$, and (*c*) $\delta^{15}N$. Values are given as mean ± standard error, with $n = 5$. Figure is provided in colour online.

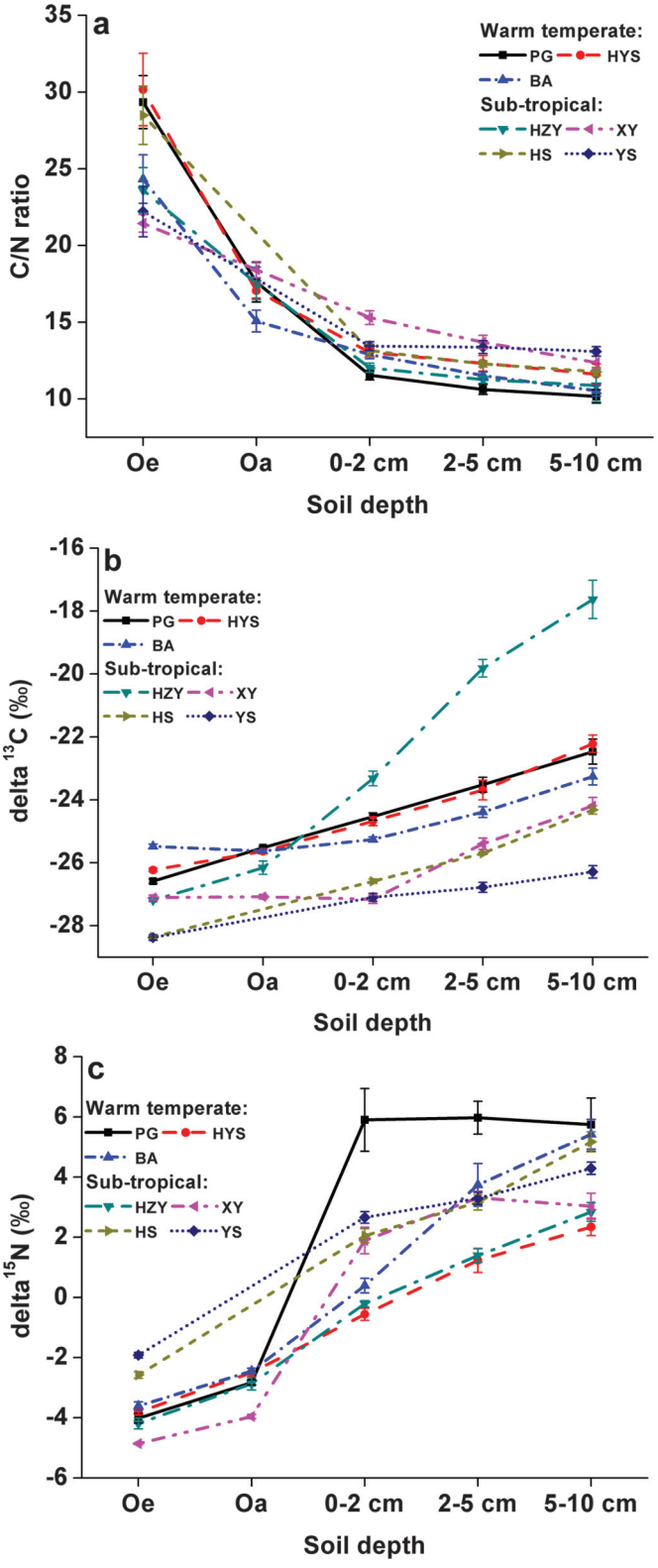

4.2. SOC composition based on NMR

The A/O ratio is widely used as an indicator of the degree of SOC degradation; however, the A/O ratio did not show consistent patterns in some studies (Blumfield et al. 2004; Lorenz et al. 2004). In the present study, among the three parts in the O-alkyl region (methoxyl, carbohydrate, di-O-alkyl), we only found a significant correlation between methoxyl C and the soil and climate variables (Table 4). Mathers et al. (2007) suggested that the presence of a large amount of lignin will protect some of the polysaccharide C from microbial attack, and thus, the O-alkyl C region may overestimate the quantity of readily decomposable C when substantial amounts of lignin are present; this might explain why the relative content of carbohydrate C in our study was not sensitive to climate and soil variables. To better investigate the links between the degree of SOC degradation and environmental variables, we evaluated the A/M ratio. Showing similar patterns across sites, the A/M ratio had closer associations with soil and climatic factors than the A/O ratio (Table 4).

The A/O ratio typically increases with progressive biodegradation of labile organic matter (OM) components (Clemente et al. 2012). Contrary to previous reports of an accumulation of alkyl C and hence an increased A/O ratio with increasing soil depth (Christensen 2001; Nierop et al. 2001), in our study, neither the A/O ratio, the A/M ratio, nor the alkyl C abundance showed any consistent variation with depth. We speculate that a low A/O ratio of root detritus, which is most abundant at these shallow depths, might contribute to this lack of depth pattern, as suggested by Norris et al. (2011). The limited depth sampling in the present study might also preclude the detection of NMR patterns that occur at greater soil depths.

Instead, we found that both the A/M and A/O ratios were apparently lower in the four northern sites for the 0–10 cm mineral soil compared with the three southern sites, suggesting that the SOC in the northern sites is less decomposed compared with the southern sites. In a comparable study along a boreal forest (*Pinus banksiana* Lamb.) transect, Norris et al. (2011) observed a higher A/O ratio in the south, and Kane et al. (2005) noted that the proportional amount of labile SOM in the mineral soil decreased with increasing temperature in boreal *Picea mariana* (Mill.) Britton, Sterns & Poggenb. forest.

The 0–10 cm mineral soil pH had a strong negative effect on both the A/M ratio and the A/O ratio across sites. Sinsabaugh (2010) stated that the laccases of white rot fungi primarily involved in lignin breakdown generally have lower pH optima (4.0–5.0), whereas the laccases of brown rot and coprophilic fungi, mainly active in polymerizing soluble phenols and thereby contributing to humification, generally have higher pH optima (6.0–7.5). With pH values ranging from 4.0 to 5.0, lignin in the 0–10 cm mineral soil at the three southern sites may be more susceptible to microbial attack than at the northern sites. We thus speculate that a faster breakdown of lignin might contribute to the higher A/M and A/O ratios in the southern sites, but further investigation is needed. Besides the strong negative effect of pH, we also observed positive relationships between MAT, MAP, and especially AET on the A/M ratio. Our finding that pH was negatively affected by MAP and AET ($r = -0.78$ and $r = -0.76$, respectively, $P < 0.05$; Table 4) suggests that differences in SOC composition involve direct impacts of soil pH plus more complex interactions between climate and soil properties.

4.3. SOC: stable isotopes and C/N ratio

Decreases in C/N ratio and increases in $\delta^{13}C$ and $\delta^{15}N$ values with depth are suggestive of increasing SOC stabilization with depth in our sites. One commonly held theory is that the $\delta^{13}C$ increases with depth are reflective of isotopic discrimination that occurs during microbial decomposition (Garten 2006; Nadelhoffer and Fry 1988), whereby microbes consume SOC, respire the light isotope (^{12}C), and incorporate the heavier isotope (^{13}C) into biomass

that is subsequently deposited in the SOM complex. As this process proceeds, SOC particles decompose into smaller sizes, which then physically migrate downward (Acton et al. 2013; Kayler et al. 2011). The C/N ratio of SOM also decreases with progressive biodegradation because plant-derived OM contains less N than microbial-derived OM (Baumann et al. 2009). Thus, as plant material is degraded, the proportion of C declines and N increases (Simpson and Simpson 2012).

With one exception (site HZY) soil $\delta^{13}C$ values were higher in the temperate zone than in the subtropical sites for a given horizon (Fig. 3*b*). Grass understory vegetation beneath *Q. variabilis* was only observed in subtropical site HZY; thus, the exceptionally high $\delta^{13}C$ there might be explained by a historical influence of C_4 grasses contributing to SOC, as $\delta^{13}C$ is much higher for C_4 than C_3 plant tissue (Vitorello et al. 1989). A simple interpretation of the slightly lower $\delta^{13}C$ in the other subtropical than the temperate sites is not possible, as Balesdent et al. (1993) indicated wide variation in tree tissue $\delta^{13}C$ within a single climatic region. However, in the present study, leaf $\delta^{13}C$ value had a strong negative relationship with MAP (R^2 = 0.91, P = 0.001; Supplementary Fig. S2[1]) and decreased from north to south. Therefore, it seems likely that differences in soil $\delta^{13}C$ between the temperate and subtropical zones reflected differences in detrital sources rather than degree of decomposition.

In summary, to our knowledge, this is the first regional investigation on SOC quantity and degree of decomposition encompassing warm temperate to subtropical forest zones with control for tree species composition. We have explored two methods to characterize the degree of SOC degradation. The NMR analysis provided the best index of degree of SOC degradation across the climatic gradient, whereas isotopic composition ($\delta^{13}C$) better reflected the degree of SOC decomposition along the soil depth gradient. Site differences in litter isotopic composition might have masked the latitudinal variation in SOC degradation. Thus, our results highlight the importance of using different techniques for characterizing SOC. No fully consistent latitudinal patterns were observed for SOC quantity. The A/M ratio, based on NMR spectra, appeared to provide the most informative index of degree of SOC decomposition. This index was strongly related to soil pH, indicating a greater degree of SOC degradation at lower soil pH in the wetter subtropical sites, which may reflect the effect of climate on pH together with the effect of pH on laccase enzymes. Further study of the interactions among macroclimate, soil development, and SOC under controlled conditions of vegetation composition could contribute to improved understanding of controls on SOC accumulation in forest soils.

Acknowledgements

We are grateful to Yunqiang Xia, Shengjun Gu, Fengjie Li, Li Zhang, Jieli Wu, Bona Dai, Xuyi Zhang, and Baoming Du for their assistance in fieldwork and laboratory analyses. We thank the two anonymous reviewers for their comments that improved the clarity of the manuscript. This work was financially supported by the National Natural Science Foundation of China (No. 31270491), SJTU Agri-X funding (No. Agri-X2015004), and SJTU SMC-B.

References

Acton, P., Fox, J., Campbell, E., Rowe, H., and Wilkinson, M. 2013. Carbon isotopes for estimating soil decomposition and physical mixing in well-drained forest soils. J. Geophys. Res. Biogeosci. **118**(4): 1532–1545. doi:10.1002/2013JG002400.

Baldock, J., Oades, J., Nelson, P., Skene, T., Golchin, A., Clarke, P., Skjemstad, J., Bell, M., and Bridge, B. 1997. Assessing the extent of decomposition of natural organic materials using solid-state ^{13}C NMR spectroscopy. Aust. J. Soil Res. **35**(5): 1061–1084. doi:10.1071/S97004.

Balesdent, J., Girardin, C., and Mariotti, A. 1993. Site-related $\delta^{13}C$ of tree leaves and soil organic matter in a temperate forest. Ecology, **74**: 1713–1721. doi:10.2307/1939930.

Baumann, K., Marschner, P., Smernik, R.J., and Baldock, J.A. 2009. Residue chemistry and microbial community structure during decomposition of eucalypt, wheat and vetch residues. Soil Biol. Biochem. **41**(9): 1966–1975. doi:10.1016/j.soilbio.2009.06.022.

Berg, B. 2000. Litter decomposition and organic matter turnover in northern forest soils. For. Ecol. Manage. **133**(1): 13–22. doi:10.1016/S0378-1127(99)00294-7.

Blumfield, T.J., Xu, Z.H., Mathers, N.J., and Saffigna, P.G. 2004. Decomposition of nitrogen-15 labeled hoop pine harvest residues in subtropical Australia. Soil Sci. Soc. Am. J. **68**(5): 1751–1761. doi:10.2136/sssaj2004.1751.

Carter, M.R. 2002. Soil quality for sustainable land management: organic matter and aggregation interactions that maintain soil functions. Agron. J. **94**: 38–47. doi:10.2134/agronj2002.0038.

Carter, M.R., Gregorich, E.G., Angers, D.A., Donald, R.G., and Bolinder, M.A. 1998. Organic C and N storage, and organic C fractions, in adjacent cultivated and forested soils of eastern Canada. Soil Tillage Res. **47**: 253–261. doi:10.1016/S0167-1987(98)00114-7.

Christensen, B.T. 2001. Physical fractionation of soil and structural and functional complexity in organic matter turnover. Eur. J. Soil Sci. **52**(3): 345–353. doi:10.1046/j.1365-2389.2001.00417.x.

Clemente, J.S., Gregorich, E.G., Simpson, A.J., Kumar, R., Courtier-Murias, D., and Simpson, M.J. 2012. Comparison of nuclear magnetic resonance methods for the analysis of organic matter composition from soil density and particle fractions. Environ. Chem. **9**(1): 97–107. doi:10.1071/EN11096.

Ding, B.Y. 2013. Citing online sources: the calculation method of evapotranspiration. Available from http://www.docin.com/p-596310449.html [accessed 29 January 2016].

Du, B., Kang, H., Pumpanen, J., Zhu, P., Yin, S., Zou, Q., Wang, Z., Kong, F., and Liu, C. 2014. Soil organic carbon stock and chemical composition along an altitude gradient in the Lushan Mountain, subtropical China. Ecol. Res. **29**(3): 433–439. doi:10.1007/s11284-014-1135-4.

Elliott, E.T., Heil, J.W., Kelly, E.F., and Monger, H.C. 1999. Soil structural and other physical properties. In Standard soil methods for long-term ecological research. Oxford University Press, New York, NY. pp. 78–80.

Eswaran, H., Van Den Berg, E., and Reich, P. 1993. Organic carbon in soils of the world. Soil Sci. Soc. Am. J. **57**(1): 192–194. doi:10.2136/sssaj1993.03615995005700010034x.

Garten, C.T., Jr. 2006. Relationships among forest soil C isotopic composition, partitioning, and turnover times. Can. J. For. Res. **36**(9): 2157–2167. doi:10.1139/x06-115.

Goodale, C.L., Apps, M.J., Birdsey, R.A., Field, C.B., Heath, L.S., Houghton, R.A., Jenkins, J.C., Kohlmaier, G.H., Kurz, W., Liu, S.R., Nabuurs, G.J., Nilsson, S., and Shvidenko, A.Z. 2002. Forest carbon sinks in the Northern Hemisphere. Ecol. Appl. **12**(3): 891–899. doi:10.1890/1051-0761(2002)012[0891:FCSITN]2.0.CO;2.

Guillaume, T., Damris, M., and Kuzyakov, Y. 2015. Losses of soil carbon by converting tropical forest to plantations: erosion and decomposition estimated by $\delta^{13}C$. Glob. Chang. Biol. **21**(9): 3548–3560. doi:10.1111/gcb.12907.

Hobbie, S.E., Reich, P.B., Oleksyn, J., Ogdahl, M., Zytkowiak, R., Hale, C., and Karolewski, P. 2006. Tree species effects on decomposition and forest floor dynamics in a common garden. Ecology, **87**(9): 2288–2297. doi:10.1890/0012-9658(2006)87[2288:TSEODA]2.0.CO;2.

Jandl, R., Lindner, M., Vesterdal, L., Bauwens, B., Baritz, R., Hagedorn, F., Johnson, D.W., Minkkinen, K., and Byrne, K.A. 2007. How strongly can forest management influence soil carbon sequestration? Geoderma, **137**(3–4): 253–268. doi:10.1016/j.geoderma.2006.09.003.

Johnsen, K.H., Samuelson, L.J., Sanchez, F.G., and Eaton, R.J. 2013. Soil carbon and nitrogen content and stabilization in mid-rotation, intensively managed sweetgum and loblolly pine stands. For. Ecol. Manage. **302**: 144–153. doi:10.1016/j.foreco.2013.03.016.

Kane, E.S., Valentine, D.W., Schuur, E.A.G., and Dutta, K. 2005. Soil carbon stabilization along climate and stand productivity gradients in black spruce forests of interior Alaska. Can. J. For. Res. **35**(9): 2118–2129. doi:10.1139/x05-093.

Kang, H., Liu, C., Yu, W., Wu, L., Chen, D., Sun, X., Ma, X., Hu, H., and Zhu, X. 2011. Variation in foliar $\delta^{15}N$ among oriental oak (*Quercus variabilis*) stands over eastern China: patterns and interactions. J. Geochem. Explor. **110**(1): 8–14. doi:10.1016/j.gexplo.2011.02.002.

Kayler, Z.E., Kaiser, M., Gessler, A., Ellerbrock, R.H., and Sommer, M. 2011. Application of $\delta^{13}C$ and $\delta^{15}N$ isotopic signatures of organic matter fractions sequentially separated from adjacent arable and forest soils to identify carbon stabilization mechanisms. Biogeosciences, **8**(10): 2895–2906. doi:10.5194/bg-8-2895-2011.

Kögel-Knabner, I., Ekschmitt, K., Flessa, H., Guggenberger, G., Matzner, E., Marschner, B., and von Lüetzow, M. 2008. An integrative approach of organic matter stabilization in temperate soils: linking chemistry, physics, and biology. J. Plant Nutr. Soil Sci. **171**(1): 5–13. doi:10.1002/jpln.200700215.

Laganiere, J., Pare, D., Bergeron, Y., Chen, H.Y.H., Brassard, B.W., and Cavard, X. 2013. Stability of soil carbon stocks varies with forest composition in the Canadian Boreal Biome. Ecosystems, **16**(5): 852–865. doi:10.1007/s10021-013-9658-z.

Lin, Y., Sun, J., and Zhang, D. 2009. Characteristics of soil fauna community in forest floor at different climate zone, China. Acta Ecol. Sin. **29**(6): 2938–2944.

Liski, J., Ilvesniemi, H., Mäkelä, A., and Westman, C.J. 1999. CO_2 emissions from soil in response to climatic warming are overestimated: the decomposition of old soil organic matter is tolerant of temperature. Ambio, **28**: 171–174.

Lorenz, K., Preston, C.M., Krumrei, S., and Feger, K.H. 2004. Decomposition of needle/leaf litter from Scots pine, black cherry, common oak and European beech at a conurbation forest site. Eur. J. For. Res. **123**(3): 177–188. doi:10.1007/s10342-004-0025-7.

Mathers, N.J., Jalota, R.K., Dalal, R.C., and Boyd, S.E. 2007. ^{13}C-NMR analysis of decomposing litter and fine roots in the semi-arid Mulga Lands of southern Queensland. Soil Biol. Biochem. **39**(5): 993–1006. doi:10.1016/j.soilbio.2006.11.009.

Meentemeyer, V. 1978. Macroclimate and lignin control of litter decomposition rates. Ecology, **59**(3): 465–472. doi:10.2307/1936576.

Nadelhoffer, K., and Fry, B. 1988. Controls on natural nitrogen-15 and carbon-13 abundances in forest soil organic matter. Soil Sci. Soc. Am. J. **52**(6): 1633–1640. doi:10.2136/sssaj1988.03615995005200060024x.

Nielsen, G.A., and Hole, F.D. 1964. Earthworms and the development of coprogenous A1 horizons in forest soils of Wisconsin. Soil Sci. Soc. Am. J. **28**(3): 426–430. doi:10.2136/sssaj1964.03615995002800030037x.

Nierop, K.G.J., van Lagen, B., and Buurman, P. 2001. Composition of plant tissues and soil organic matter in the first stages of a vegetation succession. Geoderma, **100**(1–2): 1–24. doi:10.1016/S0016-7061(00)00078-1.

Norris, C.E., Quideau, S.A., Bhatti, J.S., and Wasylishen, R.E. 2011. Soil carbon stabilization in jack pine stands along the Boreal Forest Transect Case Study. Glob. Chang. Biol. **17**(1): 480–494. doi:10.1111/j.1365-2486.2010.02236.x.

Pendall, E., Bridgham, S., Hanson, P.J., Hungate, B., Kicklighter, D.W., Johnson, D.W., Law, B.E., Luo, Y.Q., Megonigal, J.P., Olsrud, M., Ryan, M.G., and Wan, S.Q. 2004. Below-ground process responses to elevated CO_2 and temperature: a discussion of observations, measurement methods, and models. New Phytol. **162**(2): 311–322. doi:10.1111/j.1469-8137.2004.01053.x.

Quideau, S., Anderson, M., Graham, R., Chadwick, O., and Trumbore, S. 2000. Soil organic matter processes: characterization by ^{13}C NMR and ^{14}C measurements. For. Ecol. Manage. **138**(1): 19–27. doi:10.1016/S0378-1127(00)00409-6.

Schmidt, M.W.I., Torn, M.S., Abiven, S., Dittmar, T., Guggenberger, G., Janssens, I.A., Kleber, M., Kögel-Knabner, I., Lehmann, J., Manning, D.A.C., Nannipieri, P., Rasse, D.P., Weiner, S., and Trumbore, S.E. 2011. Persistence of soil organic matter as an ecosystem property. Nature, **478**(7367): 49–56. doi:10.1038/nature10386.

Schneckenberger, K., and Kuzyakov, Y. 2007. Carbon sequestration under *Miscanthus* in sandy and loamy soils estimated by natural ^{13}C abundance. J. Plant Nutr. Soil Sci. **170**(4): 538–542. doi:10.1002/jpln.200625111.

Simpson, M.J., and Simpson, A.J. 2012. The chemical ecology of soil organic matter molecular constituents. J. Chem. Ecol. **38**(6): 768–784. doi:10.1007/s10886-012-0122-x.

Simpson, M.J., Otto, A., and Feng, X.J. 2008. Comparison of solid-state carbon-13 nuclear magnetic resonance and organic matter biomarkers for assessing soil organic matter degradation. Soil Sci. Soc. Am. J. **72**(1): 268–276. doi:10.2136/sssaj2007.0045.

Sinsabaugh, R.L. 2010. Phenol oxidase, peroxidase and organic matter dynamics of soil. Soil Biol. Biochem. **42**(3): 391–404. doi:10.1016/j.soilbio.2009.10.014.

Sjogersten, S., Turner, B.L., Mahieu, N., Condron, L.M., and Wookey, P.A. 2003. Soil organic matter biochemistry and potential susceptibility to climatic change across the forest-tundra ecotone in the Fennoscandian mountains. Glob. Chang. Biol. **9**(5): 759–772. doi:10.1046/j.1365-2486.2003.00598.x.

Tavakkoli, E., Rengasamy, P., Smith, E., and McDonald, G.K. 2015. The effect of cation–anion interactions on soil pH and solubility of organic carbon. Eur. J. Soil Sci. **66**(6): 1054–1062. doi:10.1111/ejss.12294.

Vitorello, V.A., Cerri, C.C., Victória, R., Andreux, F., and Feller, C. 1989. Organic matter and natural carbon-13 distribution in forested and cultivated oxisols. Soil Sci. Soc. Am. J. **53**(3): 773–778. doi:10.2136/sssaj1989.03615995005300030024x.

von Lützow, M., Kögel-Knabner, I., Ekschmitt, K., Matzner, E., Guggenberger, G., Marschner, B., and Flessa, H. 2006. Stabilization of organic matter in temperate soils: mechanisms and their relevance under different soil conditions — a review. Eur. J. Soil Sci. **57**(4): 426–445. doi:10.1111/j.1365-2389.2006.00809.x.

Wang, Q.K., Wang, S.L., and Zhong, M.C. 2013. Ecosystem carbon storage and soil organic carbon stability in pure and mixed stands of *Cunninghamia lanceolata* and *Michelia macclurei*. Plant Soil, **370**(1–2): 295–304. doi:10.1007/s11104-013-1631-2.

Whitby, T.G., and Madritch, M.D. 2013. Native temperature regime influences soil response to simulated warming. Soil Biol. Biochem. **60**: 202–209. doi:10.1016/j.soilbio.2013.01.014.

Xu, X., Shi, Z., Li, D.J., Rey, A., Ruan, H.H., Craine, J.M., Liang, J.Y., Zhou, J.Z., and Luo, Y.Q. 2016. Soil properties control decomposition of soil organic carbon: Results from data-assimilation analysis. Geoderma, **262**: 235–242. doi:10.1016/j.geoderma.2015.08.038.

Yin, Y., Allen, H.E., Li, Y., Huang, C., and Sanders, P.F. 1996. Adsorption of mercury (II) by soil: effects of pH, chloride, and organic matter. J. Environ. Qual. **25**(4): 837–844. doi:10.2134/jeq1996.00472425002500040027x.

Yuste, J.C., Barba, J., Fernandez-Gonzalez, A.J., Fernandez-Lopez, M., Mattana, S., Martinez-Vilalta, J., Nolis, P., and Lloret, F. 2012. Changes in soil bacterial community triggered by drought-induced gap succession preceded changes in soil C stocks and quality. Ecol. Evol. **2**(12): 3016–3031. doi:10.1002/ece3.409.